PNAS
www.pnas.org

Supplementary Information for

CD8αα homodimers function as a co-receptor for KIR3DL1

Jie Geng and Malini Raghavan

Malini Raghavan
Email: malinir@umich.edu

This PDF file includes:

Supplementary text
Figs. S1 to S5
Tables S1 to S7

www.pnas.org/cgi/doi/10.1073/pnas.1905943116

Supplementary Information Text

Materials and Methods:

Antibodies

The following monoclonal antibodies were used in this study: Ascites of W6/32 and HC10 from the University of Michigan Hybridoma Core, which were labeled with Atto647N, purified anti-human CD8α (clone SK1; BioLegend), purified anti-human CD8α (clone C8/144B; BioLegend), AF700 or APC-Cy7-conjugated anti-human CD8α (clone SK1; BioLegend), AF594-conjugated anti-human CD8α (clone RPA-T8; BioLegend), AF700-conjugated anti-human CD8α (clone HIT8a; BioLegend), eFluor660-conjugated anti-human CD8β (clone SIDI8BEE; Invitrogen), Pacific Blue-conjugated anti-human CD3 (clone UCHT1; BioLegend), PE-Cy7-conjugated anti-human CD56 (clone CMSSB; eBioscience), FITC or AF700-conjugated anti-human IFNγ (clone B27; BioLegend), PE-conjugated anti-human CD107a (H4A3, BD Biosciences), PE-conjugated anti-human NKG2A (clone 131411; R&D systems), PE-conjugated anti-human KIR2DL1/S1/S3/S5 (clone HP-MA4; BioLegend), FITC-conjugated anti-human KIR2DL2/L3/S2 (clone DX27; BioLegend), purified anti-human KIR3DL1 (clone 177407; R&D SYSTEMS), APC-conjugated anti-human KIR3DL1 (clone DX9; BioLegend), and PE-conjugated anti-human KIR2DS4 (JJC11.6; Miltenyi Biotec.). Dead cells were excluded from flow cytometric analyses with 7-amino-actinomycin D (7-AAD; BD Biosciences) or the amine-reactive dye Aqua (405 nm, Life Technologies).

Peripheral blood mononuclear cell (PBMC) preparations, HLA genotyping and KIR3DL1 expression

PBMCs were isolated from whole blood using Ficoll-Paque density gradient centrifugation (GE Healthcare, Chicago, IL). As previously described (1), whole blood was diluted to 50 mL with 1x PBS + 2% FBS, layered over Ficoll-Paque and centrifuged at 400 x g for 30 min with no brakes. The buffy coat layer was then moved to a new tube and washed twice with 1x PBS + 2% FBS. Genomic DNA was extracted from the cells using a DNeasy Blood and Tissue kit (Qiagen, Maryland, USA) following the kit instructions and quantified by spectrometry. HLA genotyping was performed as described previously (1). The presence of KIR3DL1 was assessed by 4% agarose gel electrophoresis following PCR-SSP (2) with primers 5'-CCCTGGTGAAATCAGGAGAGAG-3' and 5'-TGTAGGTCCCTGCAAGGGCAA-3'.

Viruses and cell infections

HLA-B*57:03 in retroviral vector LIC pMSCVneo were prepared as described previously (3). The HLA-B*57:03 mutant that is deficient for binding CD8 (HLA-B*57:03-$CD8_{null}$) was made by introducing D227K/T228A mutations into HLA-B*57:03 using the QuikChange II site-directed mutagenesis kit. The primers were 5'-GGTCTCCACAAGCTCAGCCTTCTGAGTTTGGTCCTCGC-3' (forward) and 5'-GCGAGGACCAAACTCAGAAGGCTGAGCTTGTGGAGACC-3' (reverse). All primers were purchased from Invitrogen. Retroviruses were generated using BOSC cells and K562 cells (from ATCC CCL-243) were infected with HLA-B-encoding viruses or control viruses lacking HLA-B. Infected cells were selected by treatment with 1 mg/ml

G418 (Life Technologies), and maintained in 0.5 mg/ml G418. To prepare KIR3DL1 and CD8 expressing cells, Jurkat cells (Clone E6-1, a gift from Dr. Alice Telesnitsky) were infected with retrovirus encoding KIR3DL1 and then selected by treatment with 1 μg/ml puromycin (Sigma), and maintained in 0.5 μg/ml puromycin. Jurkat cells expressing KIR3DL1 (Jurkat-KIR3DL1) were further nucleofected with pCI-neo-CD8α and selected with 2 mg/ml G418. pJP1520-KIR3DL1 was obtained from DNASU (Clone ID=75056). pCI-neo-CD8α was a gift from Dr. Lei Lu (4) (Addgene plasmid # 86050; RRID: Addgene_86050).

Tetramer staining

Peptide-HLA-B complexes were prepared by treatment of leucine zipper-tethered HLA-B molecules with epitope-linked β_2m (LZ-ELBM HLA-B) (5) with PreScission protease (PsP, GE Healthcare Life Sciences) or thrombin for 2 hr at room temperature to release the tethered peptide, while peptide exchange was performed by adding HLA-B binding epitopes simultaneously with PreScission protease or thrombin. Peptide TSTLQEQIGW (TW10) was used for HLA-B*57:03, while peptide EEIPDFAFY(EY9) was used for HLA-B*44:02. HLA molecules were further dialyzed thoroughly with Amicon Ultra Centrifugal Filter Devices (Millipore) with a 10 kDa cutoff to remove unbound peptides. The peptide-exchanged monomers were verified by native-PAGE gels. Tetrameric HLA-I reagents were constructed by the addition of streptavidin conjugated to APC (Prozyme, PJ27S) at 4:1 molar ratios following the tetramerization protocol from NIH tetramer core facility. PBS + 0.5% dialyzed BSA was used as staining buffer. For CD8 and KIR3DL1 blocking, anti-CD8 (clone SK1; BioLegend) or anti-KIR3DL1 (clone 177407; R&D SYSTEMS) was incubated with PBMCs at 10 μg/ml for 15 min at room temperature. After washing once, freshly prepared tetramers were added typically at 20 μg/ml and anti-CD8-AF700 (clone HIT8a; BioLegend), anti-CD3-pacific blue (clone UCHT1; BioLegend) and anti-CD56-PE-Cy7 (clone CMSSB; eBioscience) were added at concentrations indicated by the manufactures and incubated for another 30 min at room temperature. Cells were washed 3 times and 7AAD was added as a live/dead marker and samples were then analyzed by flow cytometry on a BD FACS-Canto or -Fortessa flow cytometer. The FACS data were analyzed with FlowJo software version 10.0.8 (Tree Star, San Carlos, CA).

Cell conjugation assay

K562 cells expressing HLA-B*57:03, HLA-B*57:03-CD8null or lacking HLA-I (those infected with a control virus) were first labeled with CFSE according to manufacturer's protocol. CFSE-labeled K562 cells were incubated with Jurkat-KIR3DL1-CD8 cells at 1:1 in complete RPMI 1640 medium with 10% FBS at 37 ^{o}C incubator for 1 hr after centrifuge (400 x g) for 5 minutes. The cells were then washed with 1X PBS, fixed with 4% PFA and stained with anti-CD8-AF700 (SK1, BioLegend). CFSE and $CD8^+$ double positive cells were quantified by flow cytometry as conjugated cells. The cell number ratio of $CFSE^+CD8^+$ / total $CFSE^+$ was used to calculate the fraction of K562 cells conjugated to Jurkat-KIR3DL1-CD8 cells as an indicator of the conjugation tendency.

KIR3DL1 clustering assay

The Jurkat cells expressing KIR3DL1 and CD8 were mixed with K562 cells expressing B*57:03 or B*57:03-$CD8_{null}$, centrifuged briefly and incubated for 10 min at 37 ^{o}C to allow

immunological synapse formation. Cells were fixed and stained with anti-KIR3DL1-APC (clone DX9; BioLegend) or together with anti-CD8-AF594 (clone RPA-T8; BioLegend). Cells were then imaged using a Leica SP8 confocal microscope. Data were processed using Leica Imaging software and ImageJ software. The intensity of KIR3DL1 or CD8 at the interface was compared with the membrane at a noncontact area and plotted as the fold increase above background.

NK cell activation assays

NK cells were defined as the $CD3^{-}CD56^{+}$ cells within the lymphocyte gate using Pacific Blue-conjugated anti-human CD3 (clone UCHT1; BioLegend) and PE-Cy7-conjugated anti-human CD56 (clone CMSSB; eBioscience). NK cells were tested for their cytolytic potential based on CD107a mobilization as described (6). In this test, anti-CD107a-PE was added to PBMC and K562 cell mixtures during a 6 hr incubation. Samples were then analyzed on a BD FACS-Fortessa flow cytometer. BD stop was added during the assay. For IFNγ production detection, PBMCs were incubated with K562 cells expressing exogenous HLA-I or not for 6 hr at 37 ^{o}C in the presence of BD plug. Cells were then washed and stained for cell surface markers and IFNγ. For assays to test the effect of CD8 on NK cell activation, AF700-conjugated anti-human CD8α (clone SK1; BioLegend) and APC-conjugated anti-human KIR3DL1 (clone DX9; BioLegend) were used. For assays to test the effect of CD8 on NK cell education, previously described procedures were used (6). PE-conjugated anti-human NKG2A (clone 131411; R&D systems), PE-conjugated anti-human KIR2DL1/S1/S3/S5 (clone HP-MA4; BioLegend), FITC-conjugated anti-human KIR2DL2/L3/S2 (clone DX27; BioLegend), and PE-conjugated anti-human KIR2DS4 (JJC11.6; Miltenyi Biotec.) were used to exclude $NKG2A^{+}$ or $KIR2D^{+}$ cells and APC-conjugated anti-human KIR3DL1 (clone DX9; BioLegend), as well as AF594-conjugated anti-human CD8α (clone RPA-T8; BioLegend), was used to show the CD8 and KIR3DL1 expression. Thereafter, cells were fixed and permeabilized with 0.2% saponin. Intracellular IFNγ was detected as described above with anti-IFNγ-FITC for assays to test the effect of CD8 on NK cell activation or anti-IFNγ-AF700 for assays to test the effect of CD8 on NK cell education. For CD8 dependency study, the fraction of NK cells expressing IFNγ after K562 cell treatment was calculated for both $CD8^{+}$ cells and $CD8^{-}$ cells. All samples were analyzed on a BD FACS-Fortessa flow cytometer. The FACS data were analyzed with FlowJo software version 10.0.8 (Tree Star, San Carlos, CA). Statistical analysis were performed with paired Student's t tests.

Statistical analysis

Statistical analyses were performed using GraphPad Prism version 7.

References:

1. Yarzabek B*, et al.* (2018) Variations in HLA-B cell surface expression, half-life and extracellular antigen receptivity. *Elife* 7:e34961.
2. Kulkarni S, Martin MP, & Carrington M (2010) KIR genotyping by multiplex PCR-SSP. *Methods Mol Biol* 612:365-375.
3. Rizvi SM*, et al.* (2014) Distinct assembly profiles of HLA-B molecules. *J Immunol* 192(11):4967-4976.

4. Madugula V & Lu L (2016) A ternary complex comprising transportin1, Rab8 and the ciliary targeting signal directs proteins to ciliary membranes. *J Cell Sci* 129(20):3922-3934.
5. Geng J, Altman JD, Krishnakumar S, & Raghavan M (2018) Empty conformers of HLA-B preferentially bind CD8 and regulate $CD8^+$ T cell function. *Elife* 7:e36341.
6. Anfossi N*, et al.* (2006) Human NK cell education by inhibitory receptors for MHC class I. *Immunity* 25(2):331-342.

Fig. S1

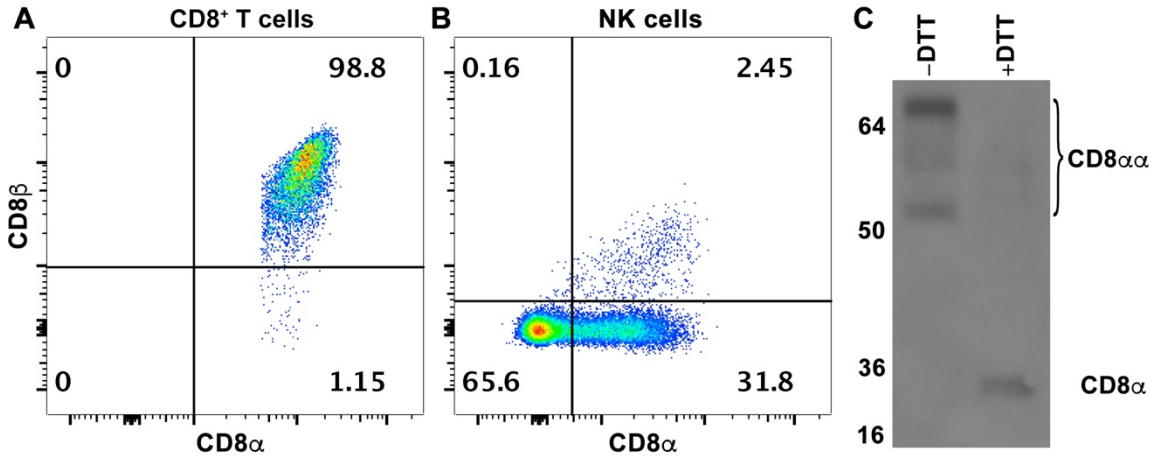

Fig. S1. CD8αα homodimers were expressed in a significant proportion of NK cells. Primary $CD8^+$ T cells (A) and NK cells (B) from PBMCs were stained with anti-CD8α and anti-CD8β. A majority of $CD8^+$ T cells ($CD3^+CD8^+$) express both CD8α and CD8β, while a majority of $CD8^+$ NK cells ($CD3^-CD56^+CD8^+$) only express CD8α. (C) Bulk NK cells purified from PBMCs were lysed and cell lysates incubated with SDS-loading buffer with or without DTT were tested by immunoblots with anti-CD8α. Monomeric CD8α (predicted molecular weight 26-35 kDa depending on post translational modifications) was present under reducing conditions, whereas non-reducing conditions gave bands in the 52-66 KDa range, suggesting that CD8α forms dimers linked by disulfide bonds. Multiple bands in Lane 1 are likely to represent differently oxidized forms of the homodimer, based on the presence of two cysteines in the stalk region, and one cysteine in the transmembrane domain.

Fig. S2

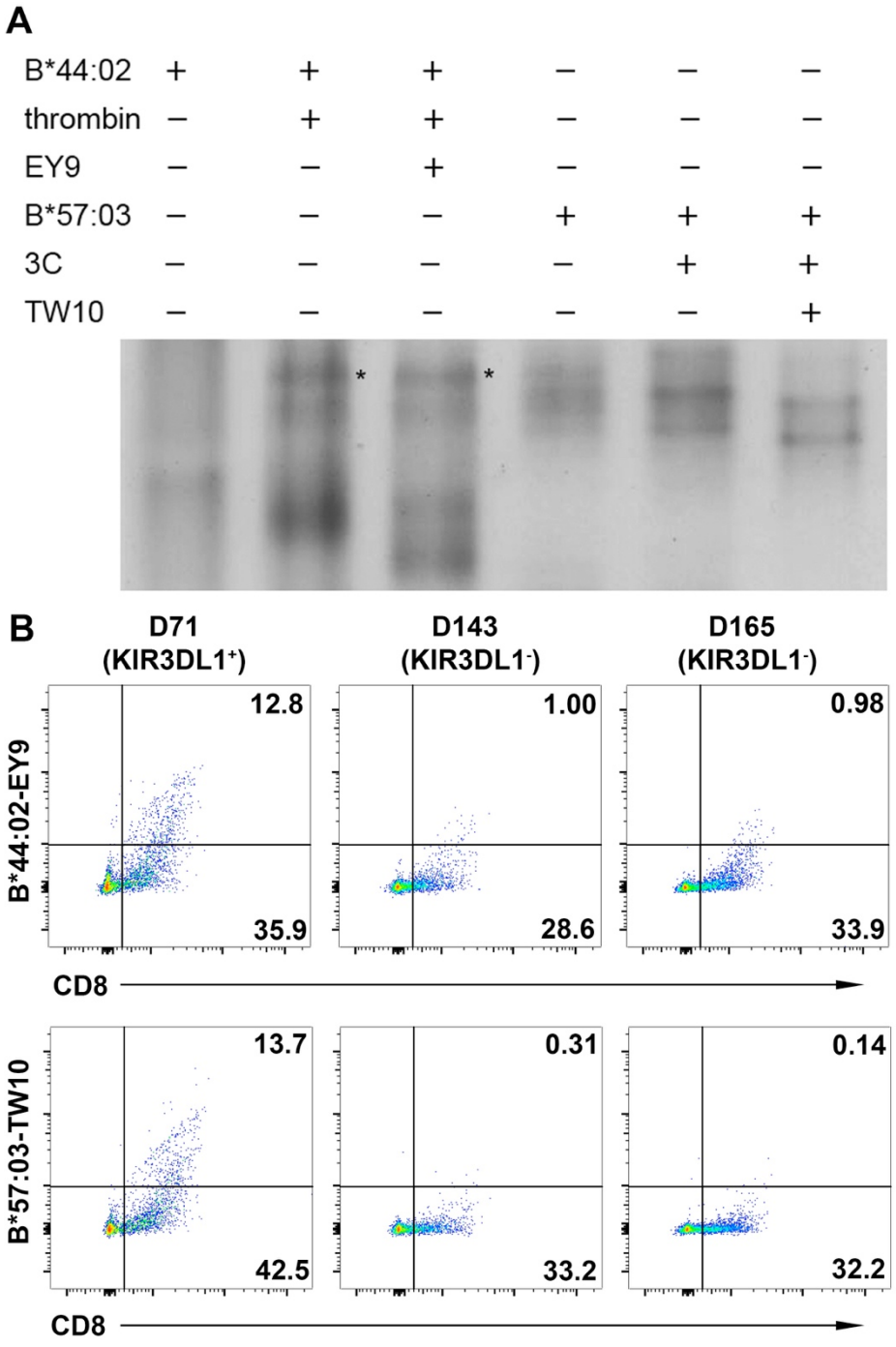

Fig. S2. (A) B*44:02-EY9 and B*57:03-TW10 were prepared by incubating ELBM versions of B*44:02 and B*57:03 with peptides EY9 and TW10 in the presence of

thrombin and PreScission protease (3C) respectively. Native gels were run to verify peptide loading. Both loaded complexes showed an increased migration rate, consistent with the negative net charge of both EY9 and TW10. *indicates the thrombin bands. (B) Only NK cells ($CD3^-CD56^+$ PBMCs) from $KIR3DL1^+$ donors (such as D71) were stained with HLA-Bw4 tetramers, while those from $KIR3DL1^-$ donors (such as D143 and D165) did not show significant HLA-Bw4 tetramer staining, suggesting that the target of the tetramer staining is KIR3DL1.

Fig. S3

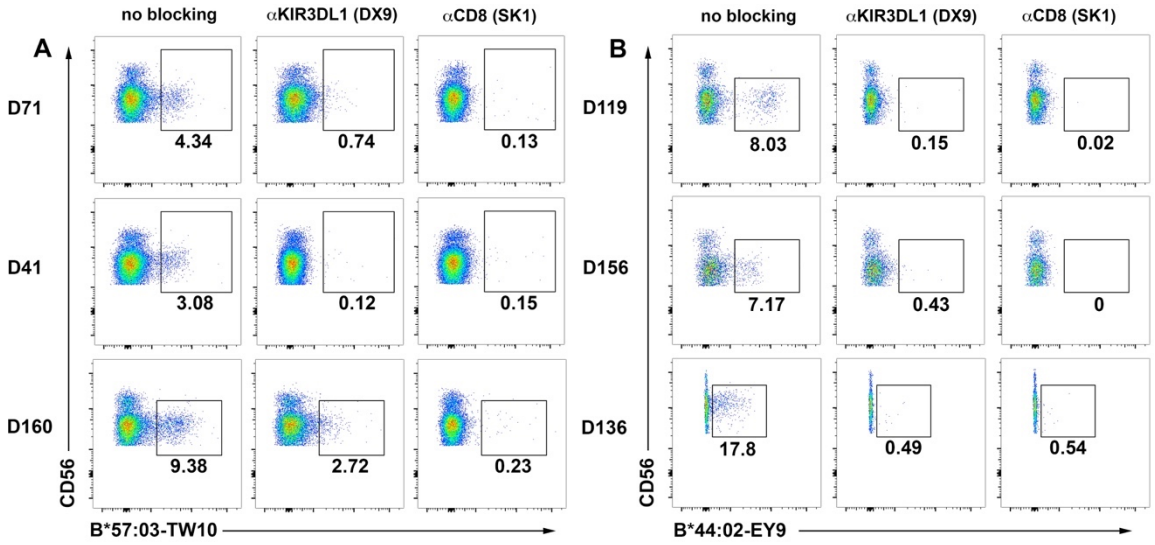

Fig. S3. Additional tetramer staining data verify that CD8 synergizes with KIR3DL1 for binding HLA-Bw4. NK cells ($CD3^{-}CD56^{+}$ PBMCs) were stained with B*57:03-TW10 (A) or B*44:02-EY9 (B) tetramers (Column I). Tetramer staining was blocked by anti-KIR3DL1 (Column II) or anti-CD8 antibodies (Column III).

Fig. S4

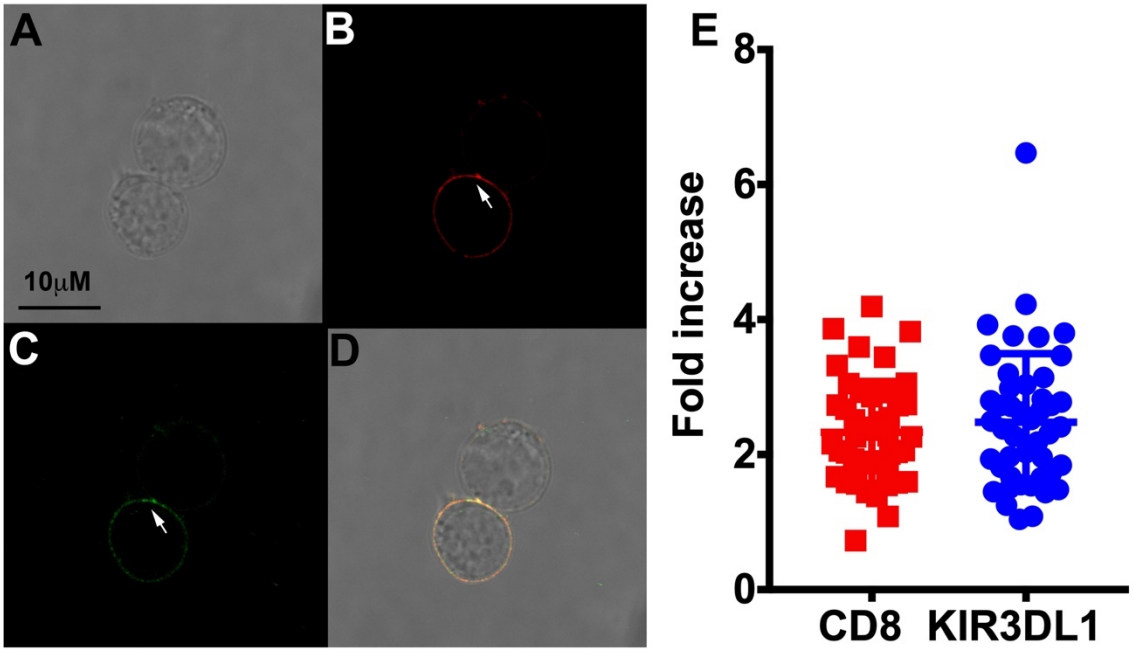

Fig. S4. Clustering of KIR3DL1 and CD8 in the immunological synapse. Jurkat-KIR3DL1-CD8 cells were incubated with K562 cells expressing B*57:03 and then fixed and stained with anti-KIR3DL1 and anti-CD8 before analysis by confocal microscopy. A: brightfield, B: CD8, C: KIR3DL1, D: merge. Arrowheads indicate clustering at the interface between the Jurkat and K562 cells. The intensity of staining of the Jurkat cells at cell-cell interfaces was compared with that measured at a noncontact area. Data are plotted as the fold increase in intensity above the non-contact area background (E). The results shown here are from two independent experiments with a total of > 40 conjugates. Data are shown as mean±S.D. Statistical analyses were performed with paired Student's *t* tests using GraphPad Prism version 7.

Fig. S5

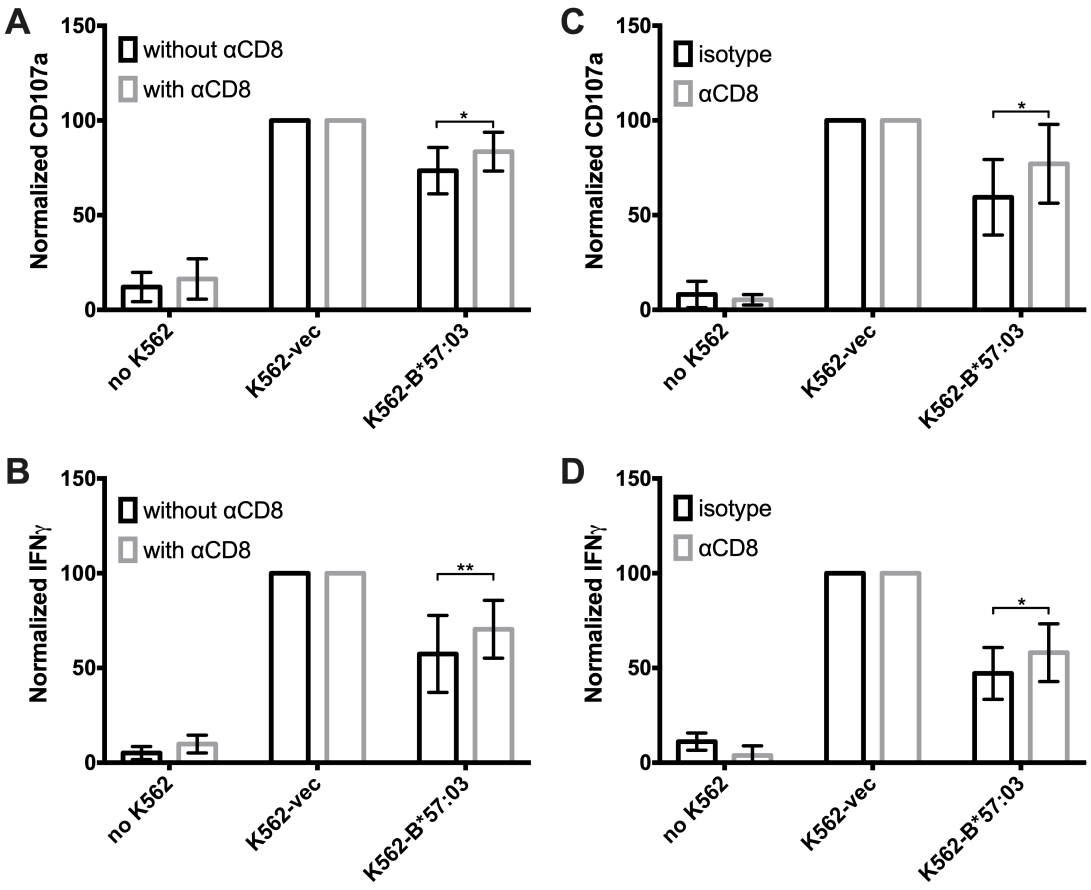

Fig. S5. Additional data showing that CD8 enhances inhibitory ability of HLA-B*57:03 to NK cell ($CD3^{-}CD56^{+}KIR3DL1^{+}$) activation through engaging KIR3DL1. Figure 3 compares effects of anti-CD8 and isotype control whereas this figure includes comparisons between conditions with anti-CD8 and conditions without any antibody. Cell activation rate was normalized to the NK cells treated with K562-vec cells after background correction (based on untreated NK cells). Data before normalization are shown in Table S4-7. *$P < 0.05$, **$P < 0.01$.

Table S1: Fraction of K562 cells in conjugation to Jurkat-KIR3DL1-CD8 cells corresponding to Fig. 2D.

	No antibody			αKIR3DL1		
	K562-vec	K562-B*57:03	K562-B*57:03-CD8 null	K562-vec	K562-B*57:03	K562-B*57:03-CD8 null
Exp1	9.73	16.10	10.68	12.05	14.3	10.86
Exp2	6.30	12.60	6.62	7.56	9.27	7.97
Exp3	6.47	7.96	6.76	5.97	6.41	6.42

Table S2: Fraction of KIR3DL1^{+} NK cells expressing CD107a corresponding to Fig. 3B.

	isotype				αCD8			
	no K562	K562-vec	K562-B*57:03	K562-B*57:03-CD8 null	no K562	K562-vec	K562-B*57:03	K562-B*57:03-CD8 null
Exp1	2.23	64.29	28.4	35.4	2.35	59.7	32.9	36.8
Exp2	4.1	12.54	6.46	9.57	2.39	13.3	7.03	7.97
Exp3	1.82	49.1	23.3	33.8	3.35	54.1	32.8	37.2
Exp4	1.02	54.4	27.55	34.8	2.84	52	32.3	34.4

Table S3: Fraction of KIR3DL1^{+} NK cells expressing IFNγ corresponding to Fig. 3D.

	isotype				αCD8			
	no K562	K562-vec	K562-B*57:03	K562-B*57:03-CD8 null	no K562	K562-vec	K562-B*57:03	K562-B*57:03-CD8 null
Exp1	3.71	68.5	25.19	35.1	5.25	59.8	27.91	32.07
Exp2	0.45	14.53	3.99	6.47	1.54	15.81	7.03	6.46
Exp3	0	49.5	19.35	26.09	1.92	48.9	28.84	28.62
Exp4	0.61	58.3	24.47	30.65	1.96	49.3	27.73	27.22

Table S4: Fraction of KIR3DL1^{+} NK cells expressing CD107a corresponding to SI Appendix, Fig. S5A.

	Without αCD8			With αCD8		
	no K562	K562-vec	K562-B*57:03	no K562	K562-vec	K562-B*57:03
Exp1	11.29	50	41.7	9.85	47.3	38.3
Exp2	7.6	52.6	40.7	5.46	44.3	40.4
Exp3	3.48	20.22	13.44	6.47	18.74	16.78
Exp4	3.31	30.83	22.19	5.31	31.02	23.51
Exp5	2.59	41.5	22.4	2.33	48.8	33.4
Exp6	1	84.33	74.03	2.66	83.38	77.43

Table S5: Fraction of KIR3DL1^{+} NK cells expressing IFNγ corresponding to SI Appendix, Fig. S5B.

	Without αCD8			With αCD8		
	no K562	K562-vec	K562-B*57:03	no K562	K562-vec	K562-B*57:03
Exp1	4.5	48.3	24.93	6.84	46.4	29.3
Exp2	0.49	42.51	19.08	2.73	39.42	22.47
Exp3	0.87	30.2	14.08	3.46	30	20.13
Exp4	1.28	49.3	36.2	1.41	49.6	40.9
Exp5	3.7	41.9	15.65	7.01	48.05	27.68
Exp6	5.13	89.18	80.7	7.34	88.6	84.3

Table S6: Fraction of KIR3DL1^{+} NK cells expressing CD107a corresponding to SI Appendix, Fig. S5C.

	isotype			αCD8		
	no K562	K562-vec	K562-B*57:03	no K562	K562-vec	K562-B*57:03
Exp1	1.42	72.4	61.7	3.99	68.2	70.2
Exp2	9.15	81.3	52.6	2.24	81.6	64.1
Exp3	1.23	43.2	17.81	3.86	43.4	32.4
Exp4	8.42	51.25	23.8	2.26	61.7	32.2

Table S7: Fraction of KIR3DL1^{+} NK cells expressing IFNγ corresponding to SI Appendix, Fig. S5D.

	isotype			αCD8		
	no K562	K562-vec	K562-B*57:03	no K562	K562-vec	K562-B*57:03
Exp1	5.53	69	44	1.99	61.7	46.91
Exp2	6.27	75.84	39.98	0	74.19	46.29
Exp3	8.57	48.2	18.2	5.79	51.9	28.14
Exp4	5.61	54.3	18.59	0.45	54.21	21.48